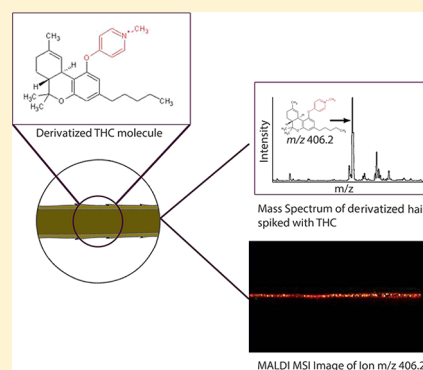


Detection and Mapping of Cannabinoids in Single Hair Samples through Rapid Derivatization and Matrix-Assisted Laser Desorption Ionization Mass Spectrometry

Emma Beasley, Simona Francese, and Tom Bassindale*

Centre for Mass Spectrometry Imaging, Biomolecular Research Centre, Sheffield Hallam University, Howard Street, S1 1WB Sheffield, United Kingdom

ABSTRACT: The sample preparation method reported in this work has permitted for the first time the application of matrix-assisted laser desorption ionization mass spectrometry (MALDI-MS) profiling and imaging for the detection and mapping of cannabinoids in a single hair sample. MALDI-MS imaging analysis of hair samples has recently been suggested as an alternative technique to traditional methods of GC/MS and LC/MS due to simpler sample preparation, the ability to detect a narrower time frame of drug use, and a reduction in sample amount required. However, despite cannabis being the most commonly used illicit drug worldwide, a MALDI-MS method for the detection and mapping of cannabinoids in a single hair has not been reported. This is probably due to the poor ionization efficiency of the drug and its metabolites and low concentration incorporated into hair. This research showed that in situ derivatization of cannabinoids through addition of an *N*-methylpyridium group resulted in improved ionization efficiency, permitting both detection and mapping of Δ^9 -tetrahydrocannabinol (THC), cannabinol (CBN), cannabidiol (CBD), and the metabolites 11-nor-9-carboxy- Δ^9 -tetrahydrocannabinol (THC-COOH), 11-hydroxy- Δ^9 -tetrahydrocannabinol (11-OH-THC), and 11-nor-9-carboxy- Δ^9 -tetrahydrocannabinol glucuronide (THC-COO-glu). Additionally, for the first time an in-source rearrangement of THC was observed and characterized in this paper, thus contributing to new and accurate knowledge in the analysis of this drug by MALDI-MS.



The use of hair as an alternative biological sample in toxicological analysis is well documented. This is due to the fact that hair offers a longer time frame to detect drug use than the more traditional blood or urine. By measuring the length of the hair and approximating the rate of hair growth (1 cm/month on average),¹ it is possible to estimate when specific drug intake occurred, over a time period as long as the length of the hair allows (weeks, months, or even years).² This is in stark contrast to blood and urine analysis, where most drugs cannot be detected beyond a few hours to days after intake.³ Some important applications of hair samples for retrospective detection of drug intake include investigating drug-facilitated crime, workplace testing, child protection cases, and therapeutic monitoring.

Hair analysis is often used to identify cannabis consumption. Cannabis continues to be the most widely used illicit drug in England and Wales, with an estimated 6.7% of adults having used cannabis in the last year,⁴ a higher percentage than the European average of 5.7%.⁵ Δ^9 -Tetrahydrocannabinol (THC) is the main psychoactive constituent of cannabis. THC undergoes a complex hepatic metabolism based on oxidation and subsequent glucuronidation.⁶ Since this enzymatic pathway is present only in vivo, metabolite detection has been suggested as a solution to external contamination problems associated with solely analyzing THC content in hair samples.¹ The main oxidative metabolites of THC are 11-hydroxy- Δ^9 -tetrahydro-

cannabinol (11-OH-THC) and 11-nor-9-carboxy- Δ^9 -tetrahydrocannabinol (THC-COOH). This molecule then undergoes glucuronidation (phase II metabolism) to form 11-nor-9-carboxy- Δ^9 -tetrahydrocannabinol glucuronide (THC-COO-glu)⁷ as shown in Figure 1. Other cannabinoids routinely analyzed in hair samples include the *Cannabis sativa* plant degradation products cannabinol (CBN) and cannabidiol (CBD).^{8–13}

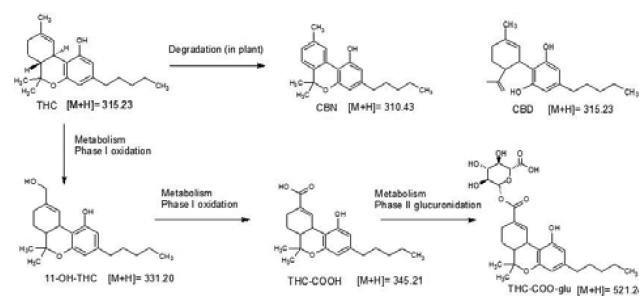


Figure 1. Degradation (ex vivo) and metabolic (in vivo) pathways of THC.

Received: September 8, 2016

Accepted: September 20, 2016

Published: September 20, 2016

THC and associated cannabinoids and metabolites can already be detected in hair samples by standard analytical techniques such as gas chromatography (GC)/mass spectrometry (MS)^{12,14–18} and liquid chromatography (LC)/MS.^{19–23} However, GC/MS requires multiple laborious and time-consuming steps before chromatographic analysis can take place, including digestion, extraction, sample cleanup, and derivatization.

LC/MS has gained in popularity over recent years, as the aforementioned derivatization step is often not needed for successful analysis. However, both methods require a large amount of hair sample (10–50 mg). GC/MS and LC/MS analyses typically give a time of intake accuracy of 1 month due to the common practice of segmenting the hair into 1 cm pieces before analysis.

More recently, direct analysis in real time (DART) has been proposed as a method for the analysis of cannabinoids and cocaine in hair samples;^{2,24} however, this method is not able to distinguish between the two isobaric species of THC and CBD, despite tandem mass spectrometric (MS/MS) analysis, because both compounds result in the same product ions. In addition to this, a large sample size is required, and currently the method is applicable only to high levels of THC associated with chronic users because the detection limit is approximately 5 ng/mg of hair. The authors stated that DART “should only be considered as a rapid pre-screening method”; however, this could result in false negative results for lower-level users.

Matrix-assisted laser desorption/ionization mass spectrometry (MALDI-MS) has been highlighted as a potential hair analysis method due to several advantages over current techniques, including improved chronological information,²⁵ simpler sample preparation, and ability to detect drugs on one single hair. Several drugs have already been analyzed in hair samples by MALDI-MS, including methamphetamine²⁶ and analogues,²⁷ cocaine,^{28–31} ketamine,³² Zolpidem,³³ and nicotine³⁴ by utilizing an α -cyano-4-hydroxycinnamic acid (CHCA) matrix without the need for analyte derivatization. Cannabis products were determined in the work of Musshof et al.,²⁹ but they were unable to determine the difference between the isobaric THC and CBD and did not look for any in vivo metabolites.

In this study, initial experiments suggested the occurrence of an in-source rearrangement of the THC molecule; in addition to low analyte ionization efficiency, this highlighted the low probability of success in mapping cannabinoids in hair samples by MALDI-MS imaging. However, the final method developed included the novel use of 2-fluoro-1-methylpyridinium *p*-toluenesulfonate (FMTPS) derivatization of hair samples in situ and showed greatly improved detection of cannabinoids and metabolites, allowing these species to be mapped by MALDI-MS imaging.

EXPERIMENTAL SECTION

Materials and Reagents. α -Cyano-4-hydroxycinnamic acid (CHCA), trifluoroacetic acid (TFA), 2-fluoro-1-methylpyridinium *p*-toluenesulfonate (FMTPS), and triethylamine (TEA) were purchased from Sigma–Aldrich. Cannabinol (CBN), cannabidiol (CBD), Δ^9 -tetrahydrocannabinol (THC), 11-nor-9-carboxy- Δ^9 -tetrahydrocannabinol (THC-COOH), 11-hydroxy- Δ^9 -tetrahydrocannabinol (11-OH-THC), Δ^9 -tetrahydrocannabinolic acid A (THCA-A), and 11-nor-9-carboxy- Δ^9 -tetrahydrocannabinol glucuronide (THC-COO-glu) were purchased as analytical references from Cerilliant (Sigma–

Aldrich). Acetonitrile (ACN) and methanol were purchased from Fisher Scientific.

Sample Preparation. CHCA was prepared at 5 mg/mL with the solvent composition being 70:30 ACN/0.2% aqueous TFA. Cannabinoid standards were mixed 1:1 with the matrix solution and deposited in triplicate on the MALDI target. The spots were left to dry at ambient temperature before analysis. Cannabinoid concentrations were 100 μ g/mL.

Derivatization of Standards for MALDI Profiling Analysis. Derivatization was carried out according to Thieme et al.³⁵ Briefly, 40 μ L of FMTPS (10 mg/mL in acetonitrile) and 10 μ L of triethylamine were mixed by vortexing. This caused the colorless solution to turn canary yellow as previously reported.^{35,36} A 20 μ L aliquot of each cannabinoid standard (100 μ g/mL) was then added, and the solutions were left at room temperature for 5 min. A sample (1 μ L) of each solution was then spotted onto a target plate.

Spiking of Hair. Hair samples from an individual who reported not using any illicit drugs were collected by cutting and washed with methanol and water by vortexing. The samples were then cut into 5 cm sections and placed into the bottom of a well in a 24-well cell culture plate in order to keep the spiking solution volume to a minimum while still submerging the hairs. The limitation of 5 cm is due to the size of a MALDI target plate. Spiked samples were prepared by soaking in 300 μ L of 0.5 μ g/mL cannabinoid standard solution. Blank hair samples were prepared by soaking in 300 μ L of methanol. The plate was sealed with tape to avoid evaporation of the standards. All hairs were soaked for 2 h, removed, and allowed to dry for 1 h at room temperature.

User Hair Sample. The hair sample collection was approved by the Sheffield Hallam University Research Ethics committee (SHU ethics number 13-2011). The hair sample was provided from a male volunteer who self-reported smoking cannabis once a week. The hairs were less than 5 cm in length. To wash, the hairs were placed in a clean test tube with methanol (5 mL) and briefly vortexed before being removed. This was repeated twice and the hairs were then left for 2 h at room temperature to dry.

In Situ Derivatization of Cannabinoids. The hair was placed on a glass slide by use of double-sided Sellotape Super Clear tape. Derivatization reagent (2.5 mL) was then sprayed by use of a Neo for Iwata airbrush at a pressure of 30 psi onto an area of 9 cm², with the sample in the center of the area. This step was carried out in a fume hood due to hazards associated with use of the triethylamine catalyst.

Deposition of Matrix for Imaging. The hairs were coated in CHCA at 5 mg/mL, with the solvent composition being 70:30 ACN/0.2% aqueous TFA, by use of the SunCollect autospraying system (SunChrom GmbH, Friedrichsdorf, Germany). Fifteen layers were sprayed at a flow rate of 2 μ L/min.

INSTRUMENTATION

MALDI Instrumentation and Analytical Conditions. All data were acquired in positive-ion mode on an Applied Biosystems/MDS Sciex hybrid quadrupole time-of-flight mass spectrometer (Q-Star Pulsar-*i*) with an orthogonal MALDI ion source (Applied Biosystems, Foster City, CA) and a neodymium-doped yttrium aluminum garnet (Nd:YAG) laser (355 nm, 1 kHz). The laser power was 30% (1000 Hz, 3.2 μ J), with an elliptical spot size of 100 \times 150 μ m.³⁷ Image acquisition was performed in raster image mode.³⁸ Decustering potential 2 was

set at 15 arbitrary units and the focusing potential at 20 arbitrary units, with an accumulation time of 0.999 s. The MALDI-MS/MS images were obtained with argon as the collision gas; the declustering potential 2 was set at 15 and the focusing potential at 20, and the collision energy and collision gas pressure were set at 20 and 5 arbitrary units, respectively.

Images were acquired with oMALDI Server 5.1 software supplied by MDS Sciex (Concord, Ontario, Canada) and processed with Biomap 3.7.5 software (www.maldi-msi.org) to generate black and white images for each m/z ratio of interest. Further image analysis and processing was performed with the public domain software ImageJ (NIH; <http://rsb.info.nih.gov/ij/>), where the previous black and white images were assigned different colors and overlaid to create one final image.

LC/MS Instrumentation and Analytical Conditions. All experiments were performed on a Thermo Finnigan LCQ classic quadrupole ion-trap liquid chromatography mass spectrometer with electrospray ionization (ESI) interfaced to a liquid chromatography system. The system used also consisted of an autosampler and autoinjector. The column used was a Phenomenex Lunar C18 (150 mm \times 1 mm, 5 μ m) with a corresponding guard column. LC/MS/MS chromatographic separation was realized by gradient elution according to a previously published method by Roth et al.³⁹ Briefly, 0.1% HCOOH in water was used as mobile phase A, and ACN + 0.1% HCOOH was used as mobile phase B. Mobile phase A was gradually reduced over time while mobile phase B was increased from 20% to 95%. The total run time was 15 min, with the THC molecule eluting at 4 min.

RESULTS AND DISCUSSION

Profiling of THC. In preliminary MALDI-MS profiling experiments, analyses were carried out on the cannabinoid standard THC as purchased from the supplier. We immediately observed a detection issue due to interference from a matrix ion peak (m/z 315.10 as seen in Figure 2A, which is more apparent at concentrations lower than 100 μ g/mL) in addition to a general low ionization yield in MALDI, as previously reported.⁴⁰ For this reason, different matrix systems were tried, including type and amount of matrix [2,5-dihydroxybenzoic acid (DHB), 6-aza-2-thiothymine (ATT), 3-hydroxycoumarin (3-HC), and 2',4',6'-trihydroxyacetophenone monohydrate (THAP)], different solvent compositions, different amounts of trifluoroacetic acid (TFA), and the addition of additives [cetrionium bromide (CTAB), lithium salts, and aniline]. In addition, negative mode analysis was conducted with 9-aminoacridine (9-AA) matrix. None of these experiments improved the detection of THC beyond that achieved with CHCA, and they will not be discussed further in this paper. Another observation from these MALDI profiling spectra was the presence of m/z peaks at 313.22 and 315.23 (Figure 2A). While the peak at 315.23 fitted the expected monoisotopic m/z of THC, the peak at 313.22 was unexplained. However, the absence of a peak at m/z 313.22 in the matrix blanks suggests that it is in fact associated with the THC molecule.

In order to investigate this phenomenon further, LC/MS/MS analysis of the THC standard (100 μ g/mL) was carried out. A single peak in the chromatogram confirmed the purity of the THC standard. Interestingly, the peak at m/z 313.22 had 3% of the intensity of the m/z 315.23 peak (seen on MALDI at approximately 110%; Figure 2A), and the isotopic peak at m/z 314.23 was no longer detected. In addition, since this LC/MS

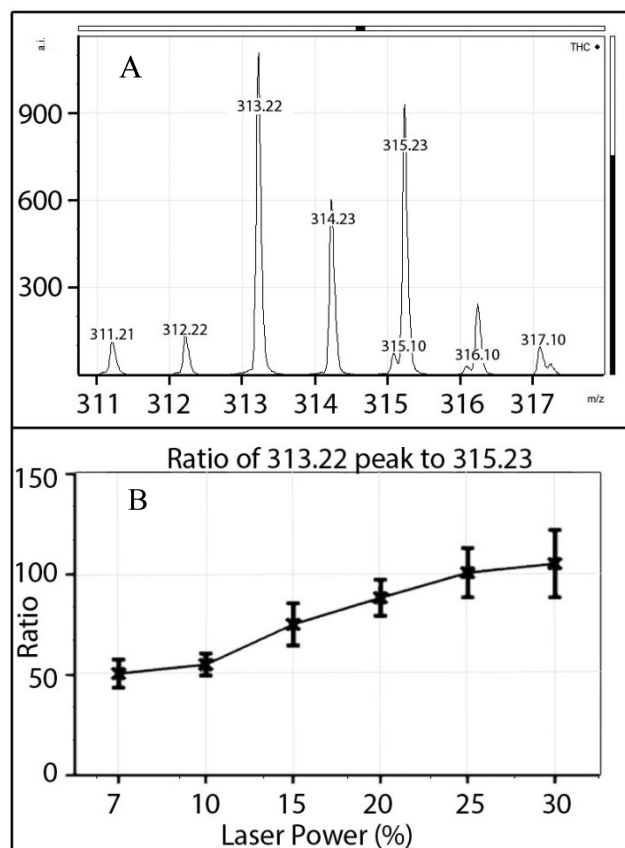


Figure 2. (A) m/z region 311–317 of THC standard with CHCA matrix. (B) Ratio of signal intensity of peaks m/z 313.22 to 315.23 at increasing laser energies.

system utilizes electrospray ionization, it is reasonable to assume that the additional peak at m/z 313.22 is specific to the MALDI ionization process, and we hypothesized that it could be dependent on the laser energy. In fact, experimentally it was observed that increasing laser power causes the ratio of m/z 313.22 to 315.23 signal intensity to increase (Figure 2B).

One possible explanation for this observation is a laser-induced rearrangement of the THC molecule. The loss of hydrogens as free radicals would increase the conjugation of the THC molecule, making it more stable and so the rearrangement would be more favorable. MS/MS spectra of m/z peaks 313.1 and 315.1 obtained by direct infusion of the THC standard also support this theory; the MS/MS spectrum of the parent ion at m/z 315.1 is shown in Figure 3A(i), and that of the rearranged parent ion at m/z 313.1 is shown in Figure 3A(ii). The spectra are very similar to many fragments formed from common mass losses (peaks labeled with stars), demonstrating that these peaks refer to the same (THC) species. Both the parent ions and many of the product ions have a mass shift of -2 Th, suggesting the loss of two hydrogens from the THC parent ion.

Bijlsma et al.⁴¹ reported the fragmentation pathway of THC-COOH, including fragments at m/z 193 and 257, based on MS^E accurate mass data. These fragments would be identical for THC-COOH and THC due to loss of the COOH group from the molecule. In this analysis the m/z 259 and 193 ions were observed in the MS/MS spectrum of the 315.1 parent ion, while we also observed a shift to m/z 257 in the MS/MS spectrum of the 313.1 parent ion. The 193 fragment was

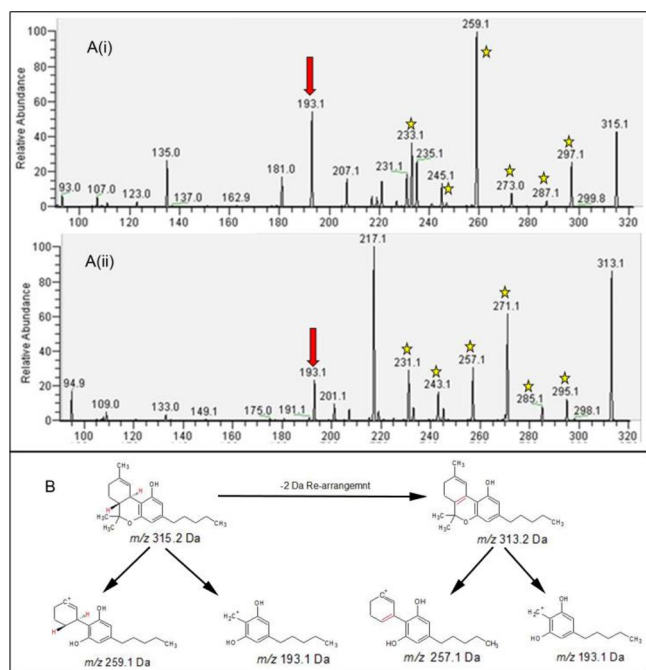


Figure 3. (A) MS/MS spectra of THC. Product ion mass spectra of (i) m/z 315 and (ii) m/z 313 are shown. Both spectra were obtained through direct infusion on an LCQ instrument. Peaks with a star symbol denote a mass shift of 2 Th. (B) Proposed rearrangement of THC and structures of fragments present at m/z 259, 257, and 193 (257 and 193 structures as proposed by Bijlsma et al.⁴¹).

present in both MS/MS spectra, indicating this fragment does not contain the proposed site of the rearrangement (see Figure 3B).

Derivatization of Cannabinoids. Once the nature of the peak at m/z 313.22 was elucidated, in order to avoid rearrangement due to the laser energy, a chemical modification of THC was carried out. Derivatization has previously been identified as a possible strategy to improve signal intensity and decrease matrix interference.^{42,43}

The target for derivatization was the hydroxyl group, since all cannabinoids of interest contain this functional group. After careful review of the literature, the derivatization method using 2-fluoro-1-methylpyridinium *p*-toluenesulfonate (FMPTS) to form an *N*-methylpyridinium derivative, as reported by Quirke et al.³⁶ for the detection of alcohols by ESI-MS, was chosen. FMPTS derivatization has previously been reported to improve the detection of a range of compounds with alcohol moieties in various sample types including surfactants,⁴⁴ estrogens,⁴⁵ and the narcotic analgesic buprenorphine,³⁵ by LC/MS analysis, and polyamides⁴² and sterols⁴⁶ in MALDI profiling experiments.

This strategy was also selected due to the simplicity of the nucleophilic substitution reaction (which occurs readily at room temperature),⁴⁷ the stability of the products formed,^{44,48} and also the addition of a permanent charge to the analytes. This is of particular importance, as it allows all cannabinoids to be analyzed in positive-ion mode (despite the nonderivatized THC-COOH being theoretically more suited to negative mode).

Derivatization was successful for all cannabinoids of interest, with all peaks being observed and in agreement with the expected monoisotopic m/z values (Table 1). The derivatized

species show an addition of 92 amu, as first reported by Quirke et al.³⁶ and confirmed by others.^{45,46}

Table 1. Theoretical and Experimental m/z Ratios for Derivatized and Nonderivatized Cannabinoid Standards

cannabinoid	[M + H]		derivatized [M + 92]	
	theor	exptl	theor	exptl
THC	315.23	315.23	406.27	406.28
CBN	311.20	311.20	402.24	402.24
CBD	315.23	315.23	406.27	406.28
11-OH-THC	331.23	331.23	422.27	422.26
THC-COOH	345.21	345.21	436.25	436.25
THC-COO-glu	521.24	521.25	612.28	612.28

After derivatization, the ions corresponding to nonderivatized cannabinoids were not observed, suggesting that reaction went to completion (or such that nonderivatized cannabinoids remained present at concentrations below the limit of detection). The expected derivatized THC peak at m/z 406.28 was the most abundant in the spectrum. However, there was evidence that rearrangement still occurred, as a peak at m/z 404.27 was observed, though it was present at only 6% of the intensity of the m/z 406.28 peak, as opposed to approximately 100% when run without derivatization. This suggests that the derivatization largely protects THC from rearrangement, possibly due to steric hindrance or increasing the required amount of laser energy to rearrange the molecule. The peak at m/z 406.28 was also observed in the mass spectrum of the derivatized CBD molecule. This was anticipated as THC and CBD are isobaric species; however, an additional peak at m/z 483.32 was also detected in the CBD spectrum; CBD gains two *N*-methylpyridinium groups, as it has one more hydroxyl group than THC. The peak at m/z 483.32 corresponds to the loss of a methyl group from the doubly derivatized molecule expected to be observed at m/z 498.32. Theoretically there could be two additions of the derivatization group to 11-OH-THC and THC-COOH and up to five additions on the THC-COO-glu molecule as a result of multiple hydroxyl groups being present, though corresponding m/z values were not observed. THC-COO-glu was detected at m/z 612.28 in the mass spectrum, corresponding to a single addition, though the peak at m/z 436.25 was much more abundant, suggesting that the glucuronide group readily fragments from the parent molecule during analysis, resulting in detection of THC-COOH. A further experiment in which the laser power used for analysis was increased showed that the ratio of THC-COO-glu to THC-COOH decreased with increasing laser power (data not shown). Another potential interferent in the assay was THCA-A, the biogenic precursor to THC. This was analyzed by the same method and showed no trace of ions relating to THC or derivatized THC (data not presented).

It was also noted that for all derivatized samples there was almost complete suppression of CHCA matrix-related peaks, as previously observed by Murgasova et al.⁴²

Imaging of Cannabinoids in Hair Samples. Once the detection of cannabinoids through derivatization was optimized, this sample preparation method was adapted to permit mapping of these species in single hair samples by MALDI-MS imaging. Preliminarily, blank and cannabinoid spiked hairs were imaged to verify efficiency of the derivatization method for

imaging purposes and were compared to hairs that had not gone through the derivatization step (Figure 4).

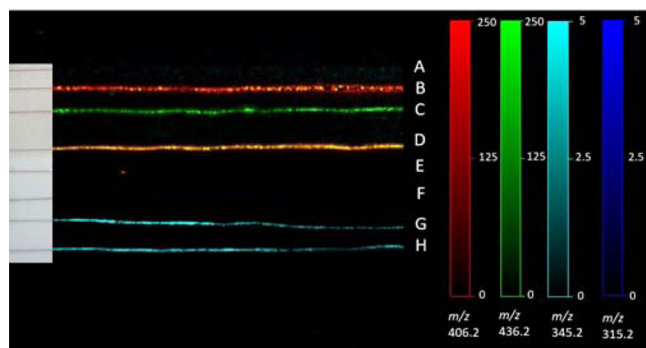


Figure 4. Comparison between (A–D) derivatized and (E–H) nonderivatized hairs: (A) soaked in methanol and derivatized, (B) soaked in THC standard and derivatized, (C) soaked in THC-COOH standard and derivatized, (D) soaked in a 1:1 mixture of THC and THC-COOH standards and derivatized, (E) soaked in methanol and not derivatized, (F) soaked in THC standard and not derivatized, (G) soaked in THC-COOH standard and not derivatized, and (H) soaked in a mixture of THC and THC-COOH standards and not derivatized.

Unless dramatic modifications are made to contrast and brightness, underivatized hairs soaked in THC standard could not be visualized in the two-dimensional (2D) molecular map, as the ion signals of underivatized THC were of extremely low intensity. Interestingly, THC-COOH could be visualized in the 2D molecular ion map (cyan) in hairs G and H, which were soaked in THC-COOH standard and a mixture of THC and THC-COOH standards, respectively; however, this was also at relatively low intensity (Figure 4). The peak at m/z 406.2, corresponding to derivatized THC, is clearly seen in hair B, which was spiked with THC and subsequently derivatized (red). Similarly, the expected ion at m/z 436.2 was observed in hair C, which was spiked with THC-COOH and subsequently derivatized (green). Hair D, which was spiked with a mixture of THC and THC-COOH and then derivatized, appears yellow in color as both THC and THC-COOH ions are present (a mixture of red and green appears yellow).

Since it was established that derivatization enhances both THC and THC-COOH signals in imaging experiments (as shown in Figure 4), a second mapping experiment with the other cannabinoids was carried out (Figure 5). The peak at m/z

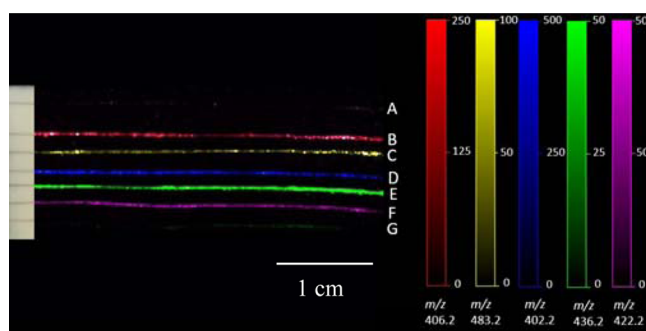


Figure 5. Simultaneous imaging of several cannabinoids of interest: hairs were soaked in (A) methanol, (B) THC, (C) CBD, (D) CBN, (E) THC-COOH, (F) 11-OH-THC, and (G) THC-COO-glu. All hairs were derivatized with FMTPS prior to analysis.

406.2, corresponding to derivatized THC, is clearly seen in hair B, which was spiked with THC and then derivatized (red); the peak at m/z 483.2 was observed in hair C, which was spiked with CBD and derivatized (yellow), the peak at m/z 402.2, corresponding to derivatized CBN, was observed in hair D, which was spiked with CBN and derivatized (blue); the peak at m/z 436.2, corresponding to derivatized THC-COOH, was observed in hair E, which was spiked with THC-COOH and derivatized (green); and finally, the peak at m/z 422.2, corresponding to derivatized 11-OH-THC, was observed in hair F, which was spiked with 11-OH-THC and derivatized (magenta). As with the profiling experiments, THC-COO-glu fragmented to give THC-COOH at m/z 436.2 (green), and its image intensity reflect a 5 \times lower concentration compared to the other standards due to the concentration in which it is supplied.

Users' hairs were investigated by the derivatization method coupled with MALDI-MS imaging, employing this optimized method. In particular, MALDI-MS/MS images were obtained of hairs collected from a volunteer who self-reported using cannabis once a week, and the transition from m/z 406.2 derivatized THC parent ion to m/z 110.0 fragment ion was monitored (Figure 6). The product ion at m/z 110.0 corresponds to the hydrated methylpyridinium fragment, which is common to all FTMPs derivatives and has previously been used for confirmation.⁴⁴

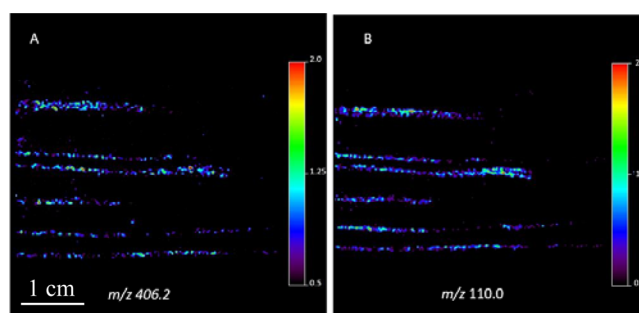


Figure 6. MS/MS image of user hairs: (A) Derivatized THC parent ion at m/z 406.2. (B) Map of fragment ion at m/z 110.

CONCLUSIONS

The use of MALDI imaging and profiling to detect cannabinoids in hair samples following in situ derivatization is presented. The method shows, for the first time, potential to detect cannabinoids from a single hair.

During the development of this method, an interesting, laser-induced THC rearrangement was observed. This caused increased fragmentation of THC and hence low ability to detect the molecule without derivatization. The novel in situ derivatization, completed in minutes at room temperature with FMTPS, showed a greatly increased limit of detection over the nonderivatized analytes and THC, CBD, CBN, and THC metabolites. The ability to detect the metabolites of THC only formed in vivo (THC-COOH, 11-OH-THC, and THC-COO-glu) will enhance the ability of the analyst to distinguish between use and unintentional exposure. During analysis, the THC-COO-glu fragments form THC-COOH, with the consequence that if m/z 436.2 is detected, it cannot be determined which of the analytes was originally present. The m/z 612 peak, however, is unique to THC-COO-glu. This is an

advantage over traditional GC/MS methods, where the glucuronide is not generally detected due to the common practice of hydrolysis or digestion of the hair sample, which converts it into THC-COOH.⁴⁹

Prior to integration into a toxicology workflow, a large sample of user hairs should be tested, from different levels of users and with different hair types. The comparison of levels of metabolites detected by traditional methods with the results from MALDI analysis will determine the limit of detection for hair samples and applicability to lower-level users, as well as the possibility of using the method quantitatively in the future. This will allow an assessment of the suitability of the method for users or whether it will be a screen for external contamination. The user hair tested here, from a regular but low-level user, provides proof that the THC at least can be detected.

The method reported has a sample preparation workflow, notwithstanding the derivatization step, that is less time-consuming, due to the lack of extraction step, than traditional GC or LC methods. This method also gives the potential to simultaneously detect THC and metabolites in a single workup and analysis. An additional advantage is the potential of MALDI-MS imaging resolution, allowing increased sensitivity to the time period of use, better than the traditional month-by-month history, although such an approach will require further validation. Analysis of hairs from a known cannabis user has shown applicability of the method to detect THC in real-life samples.

AUTHOR INFORMATION

Corresponding Author

*E-mail t.bassindale@shu.ac.uk.

Notes

The authors declare no competing financial interest.

ACKNOWLEDGMENTS

This work has been funded by a Sheffield Hallam University Vice Chancellors scholarship and the Sheffield Hallam University Biomolecular Research Centre.

REFERENCES

- (1) Cooper, G. A. A.; Kronstrand, R.; Kintz, P. *Forensic Sci. Int.* **2012**, *218*, 20–24.
- (2) Duvivier, W. F.; van Beek, T. A.; Pennings, E. J. M.; Nielen, M. W. F. *Rapid Commun. Mass Spectrom.* **2014**, *28*, 682–690.
- (3) Kintz, P. *Forensic Sci. Int.* **2012**, *218*, 28–30.
- (4) Home Office. *Drug misuse: Findings from the 2014/15 crime survey for England and Wales*, 2nd ed., 2015; https://www.gov.uk/government/uploads/system/uploads/attachment_data/file/462885/drug-misuse-1415.pdf.
- (5) European Monitoring Centre for Drugs and Drug Addiction. *European Drug Report 2015: Trends and Developments*, 2015; <http://www.emcdda.europa.eu/publications/edr/trends-developments/2015>.
- (6) Sharma, P.; Murthy, P.; Bharath, M. M. *Iran. J. Psychiatry* **2012**, *7*, 149–156.
- (7) Mazur, A.; Lichti, C. F.; Prather, P. L.; Zielinska, A. K.; Bratton, S. M.; Gallus-Zawada, A.; Finel, M.; Miller, G. P.; Radomińska-Pandya, A.; Moran, J. H. *Drug Metab. Dispos.* **2009**, *37*, 1496–1504.
- (8) Skopp, G.; Strohecker-Kuehner, P.; Mann, K.; Hermann, D. *Forensic Sci. Int.* **2007**, *170*, 46–50.
- (9) Musshoff, F.; Junker, H. P.; Lachenmeier, D. W.; Kroener, L.; Madea, B. *J. Anal. Toxicol.* **2002**, *26*, 554–560.
- (10) Strano-Rossi, S.; Chiarotti, M. *J. Anal. Toxicol.* **1999**, *23*, 7–10.
- (11) Emídio, E. S.; de Menezes Prata, V.; de Santana, F. J. M.; Dórea, H. S. *J. Chromatogr. B: Anal. Technol. Biomed. Life Sci.* **2010**, *878*, 2175–2183.
- (12) Emídio, E. S.; de Menezes Prata, V.; Dórea, H. S. *Anal. Chim. Acta* **2010**, *670*, 63–71.
- (13) Nadulski, T.; Pragst, F. *J. Chromatogr. B: Anal. Technol. Biomed. Life Sci.* **2007**, *846*, 78–85.
- (14) Pragst, F.; Balikova, M. A. *Clin. Chim. Acta* **2006**, *370*, 17–49.
- (15) Huestis, M. A.; Gustafson, R. A.; Moolchan, E. T.; Barnes, A.; Bourland, J. A.; Sweeney, S. A.; Hayes, E. F.; Carpenter, P. M.; Smith, M. L. *Forensic Sci. Int.* **2007**, *169*, 129–136.
- (16) Minoli, M.; Angeli, I.; Ravelli, A.; Gigli, F.; Lodi, F. *Forensic Sci. Int.* **2012**, *218*, 49.
- (17) Han, E.; Chung, H.; Song, J. M. *J. Anal. Toxicol.* **2012**, *36*, 195–200.
- (18) Breidi, S. E.; Barker, J.; Petróczy, A.; Naughton, D. P. *J. Anal. Methods Chem.* **2012**, *2012*, No. 907893.
- (19) Mercolini, L.; Mandrioli, R.; Protti, M.; Conti, M.; Serpelloni, G.; Raggi, M. A. *J. Pharm. Biomed. Anal.* **2013**, *76*, 119–125.
- (20) Roth, N.; Moosmann, B.; Auwärter, V. *J. Mass Spectrom.* **2013**, *48*, 227–233.
- (21) Vincenti, M.; Salomone, A.; Gerace, E.; Pirro, V. *Mass Spectrom. Rev.* **2013**, *32*, 312–332.
- (22) Thieme, D.; Sachs, H.; Uhl, M. *Drug Test. Anal.* **2014**, *6*, 112–118.
- (23) Míguez-Framil, M.; Cocho, J. Á.; Taberner, M. J.; Bermejo, A. M.; Moreda-Piñeiro, A.; Bermejo-Barrera, P. *Microchem. J.* **2014**, *117*, 7–17.
- (24) Duvivier, W. F.; van Putten, M. R.; van Beek, T. A.; Nielen, M. W. F. *Anal. Chem.* **2016**, *88*, 2489–2496.
- (25) Poetzsch, M.; Steuer, A. E.; Roemmelt, A. T.; Baumgartner, M. R.; Kraemer, T. *Anal. Chem.* **2014**, *86*, 11758–11765.
- (26) Miki, A.; Katagi, M.; Kamata, T.; Zaitso, K.; Tatsuno, M.; Nakanishi, T.; Tsuchihashi, H.; Takubo, T.; Suzuki, K. *J. Mass Spectrom.* **2011**, *46*, 411–416.
- (27) Kamata, T.; Shima, N.; Sasaki, K.; Matsuta, S.; Takei, S.; Katagi, M.; Miki, A.; Zaitso, K.; Nakanishi, T.; Sato, T.; Suzuki, K.; Tsuchihashi, H. *Anal. Chem.* **2015**, *87*, 5476–5481.
- (28) Porta, T.; Grivet, C.; Kraemer, T.; Varesio, E.; Hopfgartner, G. *Anal. Chem.* **2011**, *83*, 4266–4272.
- (29) Musshoff, F.; Arrey, T.; Strupat, K. *Drug Test. Anal.* **2013**, *5*, 361–365.
- (30) Cuypers, E.; Flinders, B.; Bosman, I. J.; Lusthof, K. J.; Van Asten, A. C.; Tytgat, J.; Heeren, R. M. A. *Forensic Sci. Int.* **2014**, *242*, 103–110.
- (31) Flinders, B.; Cuypers, E.; Zeijlemaker, H.; Tytgat, J.; Heeren, R. M. A. *Drug Test. Anal.* **2015**, *7*, 859–865.
- (32) Shen, M.; Xiang, P.; Shi, Y.; Pu, H.; Yan, H.; Shen, B. *Anal. Bioanal. Chem.* **2014**, *406*, 4611–4616.
- (33) Shima, N.; Sasaki, K.; Kamata, T.; Matsuta, S.; Katagi, M.; Miki, A.; Zaitso, K.; Sato, T.; Nakanishi, T.; Tsuchihashi, H.; Suzuki, K. *Forensic Toxicol.* **2015**, *33*, 122–130.
- (34) Uematsu, T.; Mizuno, A.; Nagashima, S.; Oshima, A.; Nakamura, M. *Br. J. Clin. Pharmacol.* **1995**, *39*, 665–669.
- (35) Thieme, D.; Sachs, H.; Thevis, M. *J. Mass Spectrom.* **2008**, *43*, 974–979.
- (36) Quirke, J. M. E.; Adams, C. L.; Van Berkel, G. *Anal. Chem.* **1994**, *66*, 1302–1315.
- (37) Trim, P. J.; Djidja, M.-C.; Atkinson, S. J.; Oakes, K.; Cole, L. M.; Anderson, D. M. G.; Hart, P. J.; Francese, S.; Clench, M. R. *Anal. Bioanal. Chem.* **2010**, *397*, 3409–3419.
- (38) Simmons, D. A. A practical introduction to MALDI-MS imaging; Applied Biosystems Technical Note, 2008; http://maldi-msi.org/wp/wp-content/uploads/2008/10/Imaging%20Overview%20Doug%20Simmons%20Sept_19_2008.pdf
- (39) Roth, N.; Moosmann, B.; Auwärter, V. *J. Mass Spectrom.* **2013**, *48*, 227–233.
- (40) Groeneveld, G.; de Puit, M.; Bleay, S.; Bradshaw, R.; Francese, S. *Sci. Rep.* **2015**, *5*, No. 11716.
- (41) Bijlsma, L.; Sancho, J. V.; Hernández, F.; Niessen, W. M. A. *J. Mass Spectrom.* **2011**, *46*, 865–875.

- (42) Murgasova, R.; Hercules, D. M.; Edman, J. R. *Macromolecules* **2004**, *37*, 5732–5740.
- (43) Bergman, N.; Shevchenko, D.; Bergquist, J. *Anal. Bioanal. Chem.* **2014**, *406*, 49–61.
- (44) Dunphy, J. C.; Pessler, D. G.; Morrall, S. W.; Evans, K. A.; Robaugh, D. A.; Fujimoto, G.; Negahban, A. *Environ. Sci. Technol.* **2001**, *35*, 1223–1230.
- (45) Lin, Y.; Chen, C.; Wang, G. *Rapid Commun. Mass Spectrom.* **2007**, *21*, 1973–1983.
- (46) Hailat, I.; Helleur, R. J. *Rapid Commun. Mass Spectrom.* **2014**, *28*, 149–158.
- (47) Mukaiyama, T.; Tanaka, T. *Chem. Lett.* **1976**, *5*, 303–306.
- (48) Adomat, H. H.; Bains, O. S.; Lubieniecka, J. M.; Gleave, M. E.; Guns, E. S.; Grigliatti, T. A.; Reid, R. E.; Riggs, K. W. *J. Chromatogr. B: Anal. Technol. Biomed. Life Sci.* **2012**, *902*, 84–95.
- (49) Kuwayama, K.; Miyaguchi, H.; Yamamuro, T.; Tsujikawa, K.; Kanamori, T.; Iwata, Y. T.; Inoue, H. *Rapid Commun. Mass Spectrom.* **2015**, *29*, 2158–2166.